We_P01_06

Penetrating Below the Diving Waves with RWI, AWI, and FWI: a NWS Australia Case Study

H.A. Debens[1]*, T. Nangoo[2], F. Mancini[1], N. Shah[2], M. Warner[2], A. Umpleby[2], M. Aitchison[2]

[1] Woodside Energy Ltd; [2] S-Cube

Summary

FWI has become a standard in velocity model building, however standalone FWI has not. To address this, FWI is brought into the model building sequence earlier by alternating RWI and AWI to recover the long-wavelength acoustic velocity model that is usually built by ray-based tomography. The corresponding long-wavelength anisotropy model is extracted using semi-global FWI. Least-squares FWI then has an adequate starting point to commence introducing the full range of length scales into the final model. The outcome is a high-resolution velocity model bypassing tomography, which penetrates over a kilometre deeper than the turning point of the deepest diving waves.

Introduction

Velocity model building (VMB) is an integral component of the seismic imaging workflow, the outputs of which underpin the vast majority of exploration and development decisions. Ray-based tomography algorithms have evolved over the last 25 years or so to become the workhorse of commercial VMB and are demonstrably effective at generating kinematically accurate velocity models (Lambaré et al. 2014). The effectiveness of this family of techniques however comes at a cost – the high-frequency approximations to the wave equation that underlie ray-based methods limit the model resolution achievable (typically to the order of the width of the first Fresnel zone), the accuracy of the model is intrinsically linked to the accuracy of picks made in the data domain, and depth-migrated domain approaches are reliant on common-image gathers containing coherent events and require careful pre-conditioning of shot gathers (demultiple, designature, etc.). Full-waveform inversion (FWI) can be considered in many respects as being the complete opposite – the resolution achievable is significantly higher (perhaps down to half the wavelength), very little manual effort is required beyond parameterising the inversion, and it operates in the shot domain and involves minimal pre-processing.

Unfortunately, this is not the whole story, as classical FWI suffers from several key limitations (cycle skipping, an inability to extract long-wavelength kinematic updates from reflection-only data, computational burden) that have prevented its widespread use. FWI's benefits, in tandem with falling costs per unit of computational throughput, have nonetheless seen it eat into the VMB workload – particularly for the shallow overburden – over the last decade. Furthermore, significant investments have been made by oil and gas, oilfield service, and technology companies to develop FWI algorithms that mitigate these limitations, thereby permitting more wholesale deployment of FWI. We present such a deployment in this paper, where a 3D anisotropic acoustic velocity model containing the full range of length scales is recovered from surface-streamer data acquired over the North West Shelf (NWS) of Australia. This is achieved using several FWI-based techniques and without the use of ray-based tomography.

Regional geology and dataset

The Pluto gas field, discovered in April 2005, sits beneath the continental shelf of Western Australia in water depths of 400 to 1000 m (Tilbury et al. 2009). The field sits between 3 and 4 km below sea level and constitutes a Triassic reservoir contained within a tilted fault block bounded by faults to the west and north. A seal is proved by overlying shales, with this sequence dipping gently to the east and subcropping against the regional Jurassic unconformity above. Numerous seafloor canyons and escarpments, along with a complex overburden, result in challenging imaging at target level.

A number of narrow-azimuth marine streamer surveys have been conducted over the field, with the most recent acquired in 2015. This survey used flip-flop air gun arrays, towed at 5 m and deployed 50 m apart, fired sequentially every 18.75 m into twelve 7-km dual-component cables towed at 20 m. The resultant data are broadband with healthy diving wave energy recorded down to roughly 2.5 km below sea level, below which a significant velocity inversion sits above the unconformity. The target is sampled by reflected energy with a limited range of scattering angles. Minimal pre-processing for inversion was applied to the data: bad traces were rejected and the amplitude spectrum limited to an acceptable range for the finite-difference kernel to be used. All free-surface effects were retained. Note that a successful reservoir-scale VMB project (travel-time tomography followed by 25 Hz FWI) over this area was delivered in 2017 by a major oilfield service company (Dickinson et al. 2017), which serves as a benchmark for the results presented here.

Methodology

The first technique used was semi-global FWI (Debens et al. 2015). This approach pairs a global inversion for long-wavelength vertical transverse isotropy (VTI) (Thomsen 1986) with conventional steepest descent FWI for vertical acoustic velocity. The initial model constructed for semi-global FWI (Figure 1a) is isotropic and extremely basic, with the idea being that this is representative of a stacking velocity generated onboard the vessel during acquisition. Only five parameters were inverted for; the first four populate the epsilon model based on user-supplied horizons, while the fifth parameter determines the epsilon/delta ratio. The horizons were picked prior to the inversion by depth migrating the raw shot gathers using the initial model.

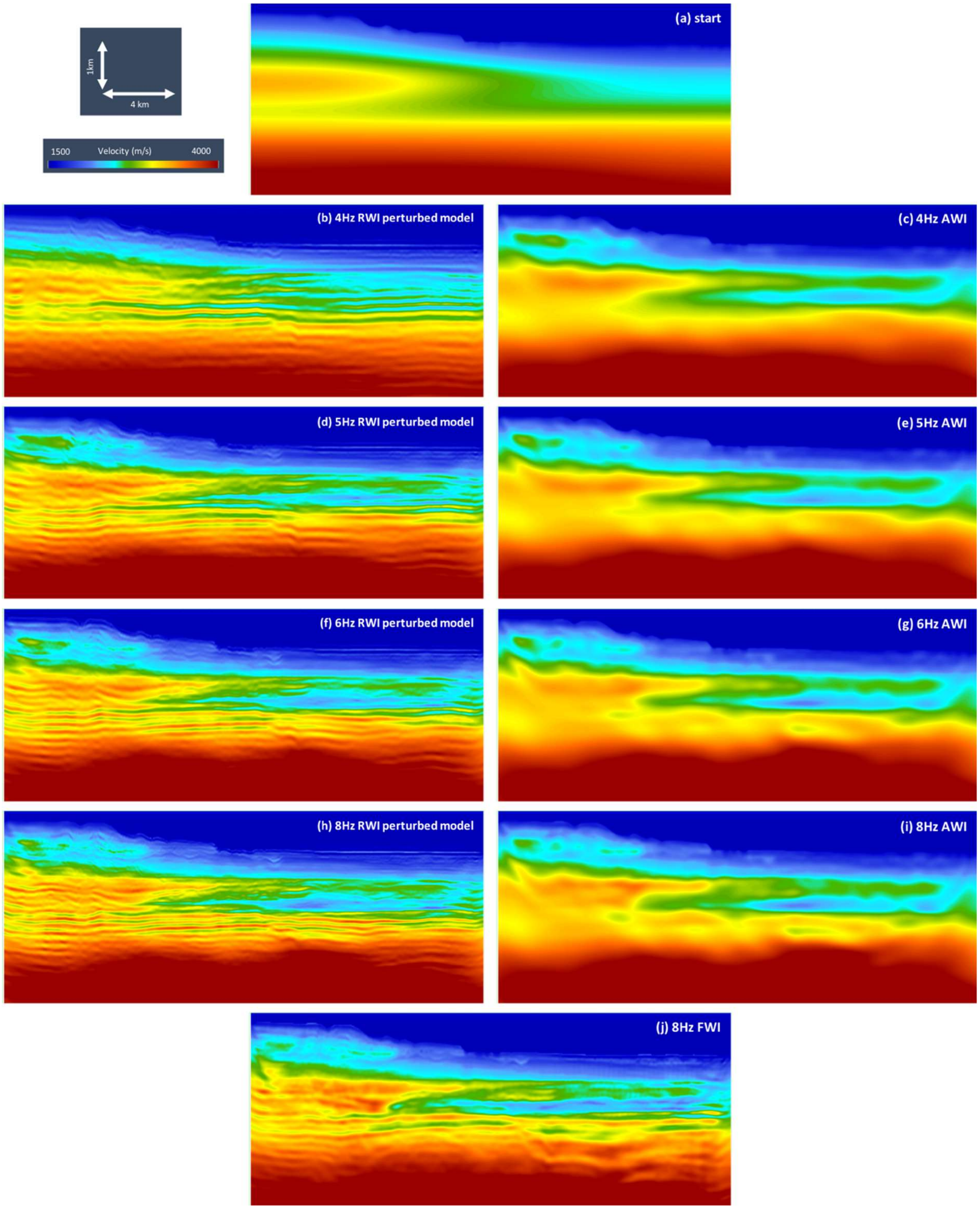

Figure 1 *The model evolution, showing the central inline section through (a) the initial model, (b)-(i) the RWI/AWI models, and (j) the FWI model. Model (j) is well resolved to over a kilometre below the zone of diving wave coverage.*

Semi-global FWI was then followed by interleaved reflection waveform inversion (RWI) and Warner and Guasch's (2016) adaptive waveform inversion (AWI), which together act to recover the long-wavelength component of acoustic velocity usually determined by travel-time tomography. The RWI stage alternates between (i) constructing a temporary high-wavenumber perturbed model for a fixed background model and (ii) computing the gradient direction with respect to the background model to minimise the residual moveout of reflected arrivals. AWI then iterates on the RWI background model update before the procedure repeats using a wider bandwidth. The RWI and AWI iterations both used the same minimally processed amplitude-normalised data. RWI focussed on the near-to-mid offset range while AWI the mid-to-long offset range. The forward modelling imposed Gardner's law for density. At each bandwidth 5 background RWI iterations were followed by 5 AWI iterations, with each iteration using 20 % of the total available shot records. Corner frequencies used were 4, 5, 6, and 8 Hz.

Finally, once an adequate model had been recovered, least-squares FWI was used to add vertical resolution and bridge the spectral gap between background and perturbed model.

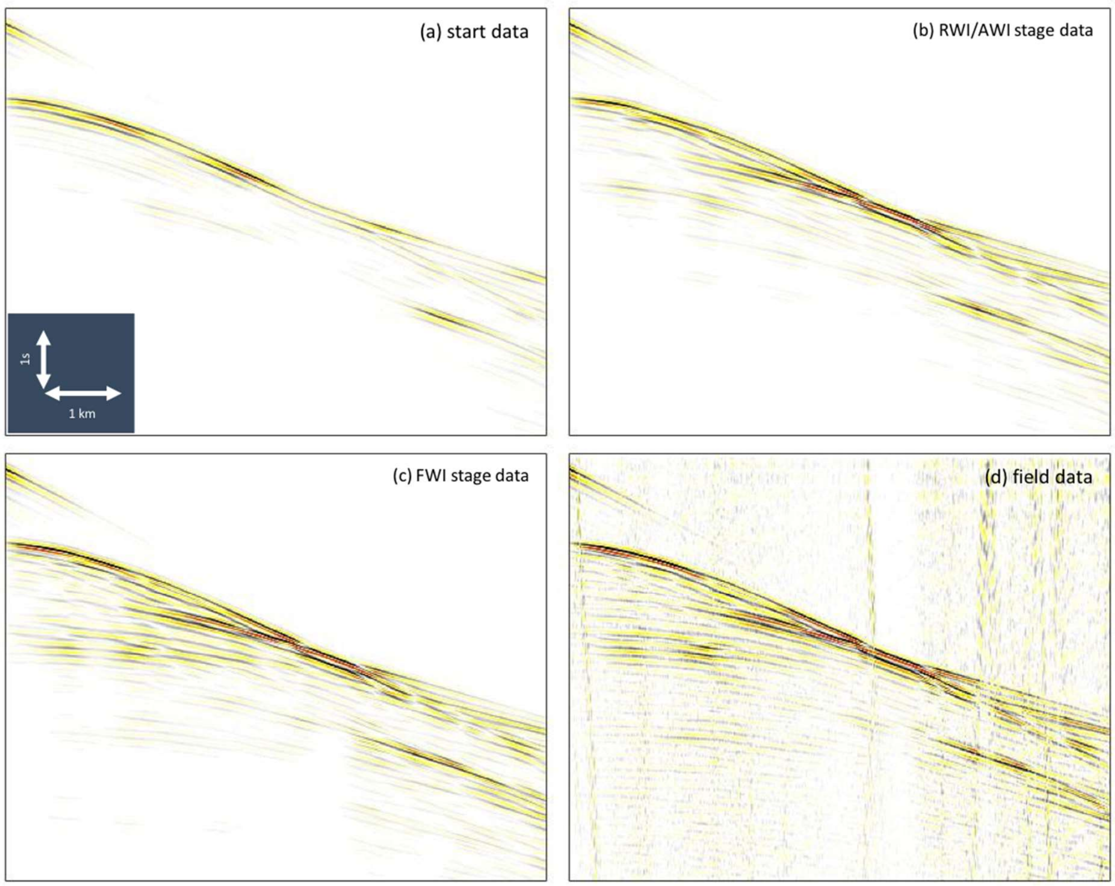

Figure 2 *The data predicted from (a) the initial model, (b) the RWI/AWI model, and (c) the FWI model, compared with (d) the field data. The reflection moveout (which drives RWI) shows a high degree of match.*

Results

The model evolution (Figure 1) shows systematic convergence with no contamination of multiples and well-matched shot gathers (Figure 2). The RWI/AWI pass can be seen to correct the macro-model, resulting in a reduction to the residual moveout of the common-image-point (CIP) gathers and remediation of several pull-downs and distortions in the stack (Figure 3). The kinematic updates penetrate over a kilometre deeper than the turning point of the deepest diving waves. The least-squares FWI pass (Figure 1j) provides geometric detail and localised velocity updates that generate strong impedance contrasts at target level.

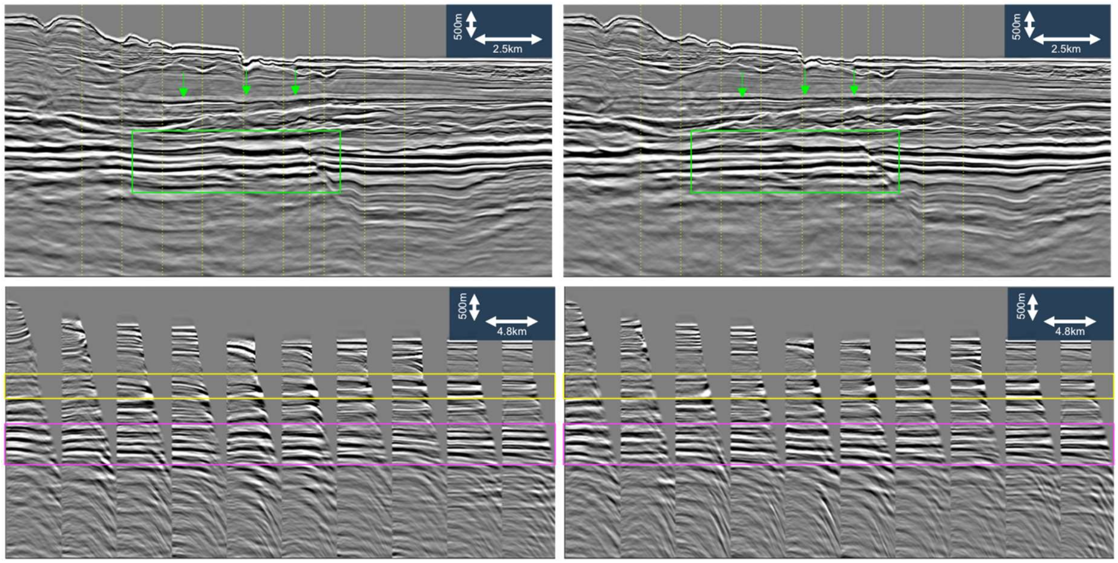

Figure 3 *Kirchhoff pre-stack depth migration full stack (top) and CIP gathers (bottom) using the initial model (left) and the RWI/AWI-updated background model (right). Noticeable improvements to several distortions in the image can be identified along with significantly flatter CIP gathers.*

Conclusions

The advantages of interleaved RWI/AWI preceding least-squares FWI are clearly demonstrated. A high-resolution anisotropic acoustic velocity model ready for imaging has been constructed from minimally processed hydrophone data without the use of high-effort travel-time tomography. The approach successfully exploits reflected arrivals to introduce both high and low wavenumbers to the model. This allows for the utilisation of FWI far earlier in the VMB workflow than conventional wisdom would suggest, leading to a significant reduction in turnaround time to the final image.

Acknowledgements

The authors would like to thank Woodside and Woodside's joint venture partners Tokyo Gas Pluto Pty Ltd and Kansai Electric Power Australia Pty Ltd for permission to present this work. They also wish to express gratitude towards the FULLWAVE Game Changer JIP at Imperial College London for their role in developing the FWI engine used. Any views or opinions expressed in this paper are solely those of the authors and do not necessarily represent those of Woodside or S-CUBE.

References

Debens, H.A., Warner, M., Umpleby, A. and da Silva, N.V. [2015] Global anisotropic 3D FWI. *SEG 2015 International Exposition and 85th Annual Meeting,* Expanded Abstracts, 1193-1197.

Dickinson, D., Mancini, F., Li, X., Zhao, K. and Ji, S. [2017] A refraction/reflection full-waveform inversion case study from North West Shelf offshore Australia. *SEG 2017 International Exposition and 87th Annual Meeting,* Expanded Abstracts, 1368-1372.

Lambaré, G., Guillaume, P. and Montel, J.P. [2014] Recent advances in ray-based tomography. *76th EAGE Conference & Exhibition*, Extended Abstracts, We G103 01.

Tilbury, L.A., Clayton, C.J., Conroy, T.J., Philip, G., Boyd, G.A., Johnson, G.A., Rayfield, M.A., Hartanto, L. and Lance, D.P. [2009] Pluto – a major gas field hidden beneath the continental slope. *The APPEA Journal*, **49**(1), 243-268.

Thomsen, L. [1986] Weak elastic anisotropy. *Geophysics*, **51**(10), 1954-1966.

Warner, M. and Guasch, L. [2016] Adaptive waveform inversion: Theory. *Geophysics*, **81**(6), R429-R445.